Available online at www.sciencedirect.com
SCIENCE DIRECT
Polymer 47 (2006) 3889–3895
polymer
www.elsevier.com/locate/polymer

Near-surface morphology effect on tack behavior of poly(styrene-*b*-butadiene-*b*-styrene) triblock copolymer/rosin films

Hoichang Yang [a], Unnyoung Sa [a], Minjeong Kang [a], Hyeon Soo Ryu [a], Chang Yeol Ryu [b], Kilwon Cho [a,*]

[a] *Department of Chemical Engineering/Polymer Research Institute, Pohang University of Science and Technology, Pohang 790-784, South Korea*
[b] *Department of Chemistry/Resselaer Nanotechnology Center, Rensselaer Polytechnic Institute, Troy, NY 12180, USA*

Received 11 August 2005; accepted 21 February 2006
Available online 18 April 2006

Abstract

The correlation between near-surface morphology and tack behavior of poly(styrene-*b*-butadiene-*b*-styrene) triblock copolymer (SBS)/rosin ester films was investigated using probe tack tests, transmission electron microscopy and small-angle X-ray scattering. The SBS/rosin films with rosin composition between 10 and 20 wt% rosin, prepared by slow evaporation of toluene during solvent casting, exhibited uniform near-surface morphology of lamellae oriented parallel to the surface. However, due to the limited solubility of rosin in the PS domains, the rosin started to phase-separate from the PS domains at 15 wt%, and formed fully separated micron-sized domains above 20 wt% rosin. The probe tack force of the SBS/rosin films increased steadily when the near-surface domain orientation changed from perpendicular cylinder to parallel lamellae on addition of rosin. Specifically, for a given lamellar morphology and surface orientation, macrophase separation of rosin plays a critical role in determining the tack properties of SBS/rosin films.

Keywords: Tack; Surface morphology; Block copolymer

1. Introduction

The tack properties of materials are important factors in determining the potential of these materials as pressure sensitive adhesives and hot melt adhesives. Elastomer-based adhesives using blends of poly(styrene-*b*-butadiene-*b*-styrene) (SBS), poly(styrene-*b*-isoprene-*b*-styrene) (SIS), or poly (styrene-*b*-ethylene-butylene-*b*-styrene) (SEBS) triblock copolymers with tackifiers have been widely studied as pressure sensitive adhesive materials [1–7]. Tack is defined as an adhesive's ability to form a physical bond with a heterogeneous surface in a shorter contact time and at a lighter pressure than required for adhesion tests [8]. Since, (shear) adhesion tests typically employ low strain rates and intermediate stress levels during contact, adhesion properties commonly reflect a large-scale deformation such as flow or plastic deformation under contact stress, over a long period of time. On the contrary, due to the relatively shorter contact times for tack tests compared to adhesion tests, pseudo-elastic deformations without macroscopic flow near the surface should play an important role in determining the tack properties [9]. In order to obtain the required tack property, adhesives must have relatively low moduli and short relaxation times to relieve internal stresses [2,10]. In such cases, low molecular weight resins are added as tackifiers to increase the flow properties and surface wettability, based on its compatibility with either the softer or harder block domains of the thermoplastic elastomer. Softer block-associating resins decrease the rubbery plateau modulus, resulting in improved tack, whereas the harder block-associating resins decrease the cohesive strength of the matrix [11].

Many studies on elastomer/tackifier blends have concentrated on balancing the ability to 'hold onto the adherend' and to 'be cleanly removed from the adherend' [1–11]. Aubrey et al. suggested that the surface energy and deformability of adhesives play an important role in the bonding and debonding process during tack tests [12]. According to Galan et al., the formation of the macrophase-separated resin domains and the tack strength of the adhesive are significantly changed by the presence of the microphase structure when either the mid or end block domains are saturated by the tackifier resins [1]. Considering the near-surface morphology of the block copolymer, the chain connectivity in block copolymers imposes limitations on

* Corresponding author. Tel.: +82 54 279 2270; fax: +82 54 279 8269.
E-mail address: kwcho@postech.ac.kr (K. Cho).

0032-3861/$ - see front matter © 2006 Elsevier Ltd. All rights reserved.
doi:10.1016/j.polymer.2006.02.081

the degrees of freedom of molecules near the polymer-air interface [13–18], and it is generally known that block chains with lower surface energy cover the free surface even when the component having higher surface energy forms the matrix [17,18]. Kim et al. found that perpendicularly oriented PS cylinders with higher surface energy exist beneath the PB layer in thermally annealed SBS thin films [16]. Hasegawa and Hashimoto observed similar behavior for SI and SB diblock copolymer blends, i.e. they found that the component with the lowest surface energy covered the free surface [17].

Our report investigates the role of near-surface morphology on tack behavior of an elastomer-based adhesive with a tackifier resin. This work shows the correlation between the tack behavior of elastomer-based adhesives and the near-surface morphologies, in particular, the micro-domain orientation and the macroscopic phase separation of the tackifier resin. An SBS triblock copolymer is used as the elastomer, and a rosin ester is used as the tackifier resin, which is selectively more miscible with PS than with PB.

2. Experimental

The SBS triblock copolymer (Kraton D1101, Shell Company) with 14 wt% SB diblock copolymer was used as a base elastomer. The molecular weight (M_w), polydispersity (PDI), and the styrene content were 136,000 g/mol, 1.15, and 33 wt% PS, respectively, [19]. The tackifier used was a commercial rosin ester (KO-90, Kolon Chemical Co., Korea), which contains a mixture of different ester branch numbers (an average of 3.8 branches, given that its average M_w is 1200 g/mol). The glass transition temperatures (T_g) of the rosin ester (50 °C), PS (98 °C) and the PB (−86 °C) domains in SBS were determined using differential scanning calorimetry (DSC).

SBS/rosin blends with rosin contents ranging from 0 to 30 wt% were prepared by solvent-casting a 5 wt% toluene solution of SBS/rosin onto 70 μm thick polyester film substrates. Then, the solvent was slowly evaporated at room temperature over a period of 7 days. Finally, the SBS/rosin films were annealed under vacuum at 120 °C for 4 days. The thickness of the resulting films was controlled to achieve 2 mm and 200 μm for rheology and probe tack tests, respectively.

The dynamic temperature sweep experiments for the SBS/rosin blends were performed in the temperature range of −120–120 °C on a Rheometrics Dynamic Spectrometer (RDS-II, Rheometrics) using parallel plates (16 mm diameter plates with a 2 mm gap), at a heating rate of 2 °C/min, an angular frequency (ω) of 1 rad/s and a strain amplitude (γ_0) of 0.5, which lies in the linear viscoelastic region.

The change in morphology of the SBS/rosin blends containing different rosin contents was observed using a transmission electron microscope (TEM) (1200EX, JEOL), operating at an accelerating voltage of 120 kV. The bulk and near-surface regions of the SBS/rosin blends were cut to approximately 50 nm thick using a cryogenic ultramicrotoming system (MT-7000, RMC). The films were first embedded using an epoxy kit (Poly/bed 812, Polysciences Inc.) for easy handling, and stained with 2 wt% osmium tetroxide (OsO_4) solution for 12 h. The stained samples were then cut using a diamond knife at −120 °C.

Small-angle X-ray scattering (SAXS) experiments for the solvent-cast and annealed SBS and SBS/rosin blends (2 mm thickness) were performed at the 4C1 beam line in Pohang Accelerator Laboratory (PAL), Korea. The wavelength λ of the incident X-ray beam was 0.1608 nm, and the distance between the sample and the 2D detector (SCX-TE/CCD-1242E, Princeton Instruments Inc.) was 180 cm. The q ($=4\pi \sin\theta/\lambda$) range was calibrated using a standard SEBS sample of well-defined structure. All SAXS profiles were normalized to the primary X-ray intensity using the signal of ionization chambers placed on either side of the sample. The 2D SAXS profiles were then converted into 1D profiles through circular averaging.

The probe tack tests on 200 μm solvent-cast SBS or SBS/rosin films were performed using a commercial probe tack tester (Texture Analyzer, Stable Micro System Ltd) in adhesion mode fitted with a 5 mm stainless steel probe. The probe contact force and time were 100 g and 10 s, respectively.

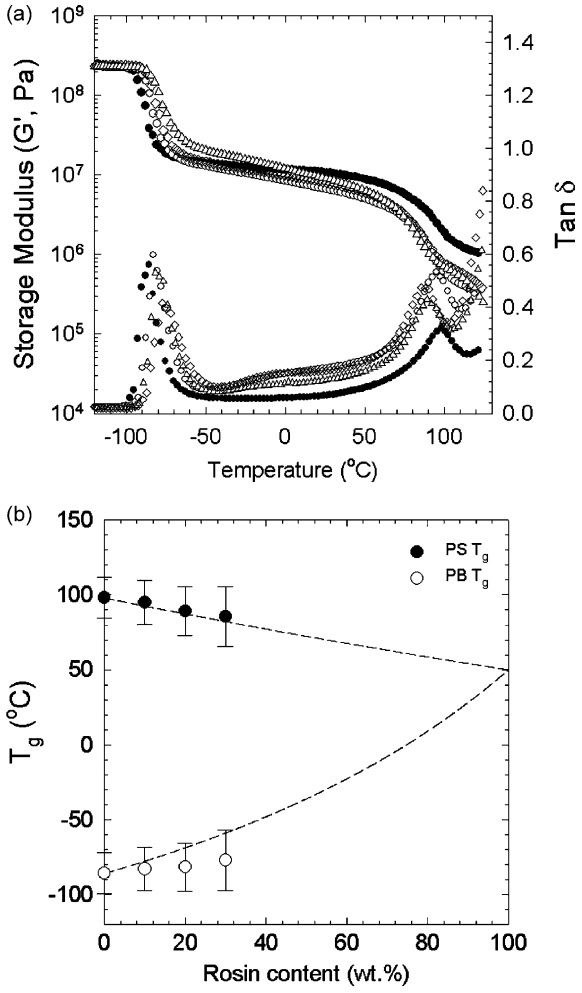

Fig. 1. (a) Storage moduli (G') and tan δ of SBS/rosin blends containing increasing rosin contents as a function of temperature (●, SBS; ○, 10 wt%; ▲, 20 wt%; ◇, 30 wt% rosin). (b) T_g values of PS and PB domains in SBS/rosin blends as a function of the rosin content. (The broken lines represent the T_g predictions by the Fox equation [20]. The error bar represents the full-width half maximum of tan δ).

The tack force was simultaneously recorded while withdrawing the probe at a rate of 10 mm/s.

3. Results and discussion

3.1. Bulk properties and morphology

To examine the viscoelastic properties of certain SBS/rosin blends, and the compatibility between SBS and the rosin at different rosin contents, linear dynamic viscoelastic moduli ($\omega = 1$ rad/s and $\gamma_0 = 0.5\%$) were measured in the temperature range from -120 to 120 °C at 2 °C/min. Fig. 1(a) represents the temperature dependence of the storage moduli (G') and tan δ of SBS/rosin blends at the indicated rosin content. The G' plateau values of the samples above glass transition temperature, T_g (PB) remained more or less unaffected, while the G' values near T_g (PS) decreased significantly as the rosin content was increased. These results correspond to a gradual decrease in

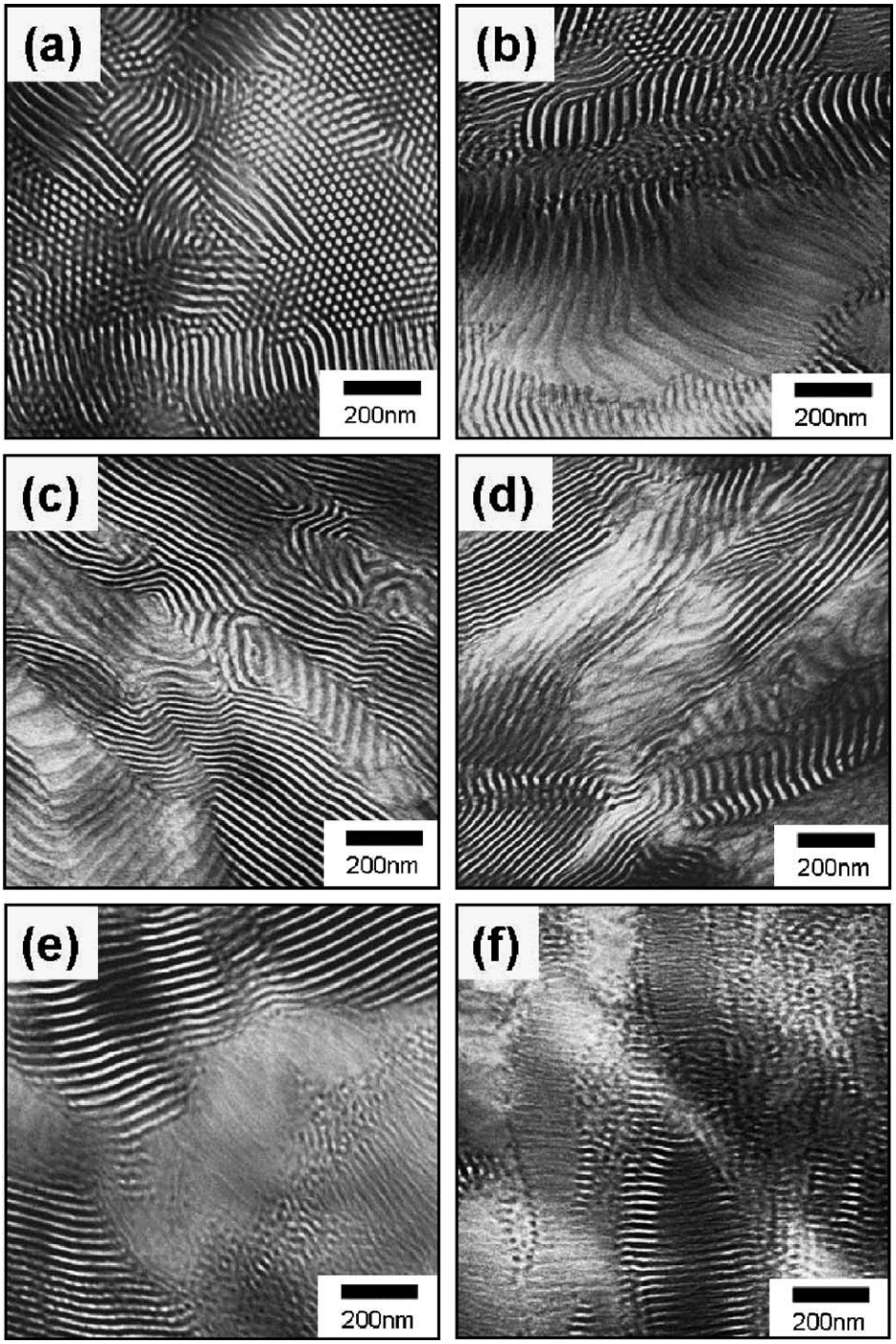

Fig. 2. TEM bulk morphologies of SBS and SBS/rosin blends containing increasing rosin contents: (a) SBS, (b) 5 wt%, (c) 10 wt%, (d) 15 wt%, (e) 20 wt%, and (f) 30 wt% rosin blend, respectively.

T_g (PS), as measured from the tan δ peak positions, according to the rosin loading in the SBS matrix. As seen in Fig. 1(b), T_g (PB) increased slightly with a broadening of the glass transition, while T_g (PS) decreased significantly as the rosin content was increased to 30 wt%. The broken lines in Fig. 1(b) represent the T_g predictions for PS/rosin and PB/rosin domains obtained from the following equation [20], respectively, assuming that T_g (PB) = −86 °C, T_g (PS) = 98 °C, and T_g (rosin) = 50 °C.

$$\frac{1}{T_g} = \frac{w_1}{T_{g1}} + \frac{w_1}{T_{g2}}$$

where T_g is the glass transition temperature of the blend, T_{g1} and T_{g2} are the glass transition temperature of the constituent components, and w_1 and w_2 are the weight fractions of the constituent components.

The measured T_g values are more in accordance with the predicted T_g (PS/rosin) values than with those obtained for T_g (PB/rosin), suggesting that rosins are more compatible with PS domains than with PB domains. Although the rosin is more miscible with PS than PB, our TEM studies showed direct evidence of macrophase separation of the rosin from SBS at higher rosin loading, which is attributed to the limited solubility of rosins in PS [1].

The selective compatibility of the rosin with PS over PB is important for controlling the ordered structures of the SBS/rosin blends. Although the rosin has limited solubility in the PS domains, its selective compatibility over PB is sufficient to induce the cylinder-to-lamellar transition upon addition of rosin. Fig. 2 shows the TEM bulk morphologies of the SBS/rosin blends containing increasing rosin contents. Since, the PB domains can be selectively stained by OsO_4 vapor, the bright and dark regions in the TEM micrographs represent the PS and PB domains, respectively. As seen in Fig. 2, the morphological transition of the SBS/rosin blends from the cylinder to lamellar phase was induced at 10 wt% rosin. For all blends with a composition higher than 10 wt% rosin, locally swollen PS/rosin and PB/rosin domains were observed, presumably due to the limited rosin solubility in the PS and PB domains. In the bulk, the appearance of micron-sized rosin domains is clearly evident when rosin contents of 20 wt% or above were used.

Since TEM only provides information on locally ordered structures, SAXS experiments were also performed to confirm the cylindrical to lamellar phase transition of the blends according to the rosin content. Fig. 3 represents the SAXS profiles for SBS and SBS/rosin blends at 25 °C. Note that all the SAXS profiles reported here are arbitrarily shifted vertically to avoid overlaps. The SAXS experiments confirmed the cylindrical to lamellar phase transition of the samples, and also identified evidence for the coexistence of cylindrical and lamellar phases (C+L) in the samples in the composition window between 10 and 20 wt% rosin. Lodge et al. studied the full phase behavior of binary mixtures of a block copolymer and a selective solvent, and concluded that ordered structures are mainly determined by the overall apparent composition of the soluble block and the selective solvent [21]. The authors reported that cylindrical to lamellar phase transition occurs

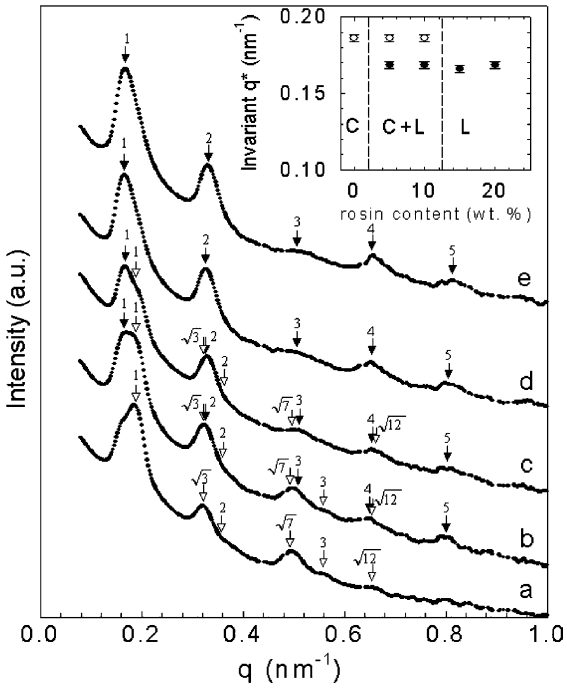

Fig. 3. SAXS profiles of SBS and SBS/rosin blends containing different rosin contents at 25 °C: (a) SBS, (b) 5wt%, (c) 10wt%, (d) and (e) 20wt% rosin, respectively. (The inset represents the invariant q^* of SBS and SBS/rosin blends as a function of the rosin content open and closed arrow-marked peaks represent C and L phases, respectively.)

upon adding dialkyl phthalates (PS selective solvents) to a PS–PI diblock copolymer. They also reported coexisting C+L phases at the phase boundary between the cylindrical and lamellar phases. It is important to note that the q maximum (q^*) position of the lamellar phase is almost invariant (Fig. 3 (inset)) upon addition of rosin above 10 wt%. This invariant q^* is attributed to the limited solubility of rosin, and it correlates closely with the bulk TEM results.

3.2. Near-surface morphology and properties

The surface organization of block copolymers is very different from the bulk form because of the thermodynamic requirements and the restrictions of these molecules on the surface [9,11,22]. Cross-sectional TEM studies of block copolymer films provide direct evidence of the near-surface morphology, but this technique demands very delicate sample treatment. To preserve the inherent surface morphology, solvent-cast SBS/rosin films (200 μm thick) were first stained by OsO_4 vapor before cutting at −120 °C. Fig. 4 represents the cross-sectional TEM micrographs of the SBS/rosin films. In all samples, the air-polymer surface is covered with a PB layer [16], showing dark or darker coloring owing to over-staining of the surface region by the OsO_4 staining agent. It was found that the near-surface morphology of the SBS/rosin films changes with increasing rosin content, as shown in the bulk. However, the morphological orientations of the microphase-separated domains near the surface are certainly different from the bulk because the polymer-air interface provides a boundary

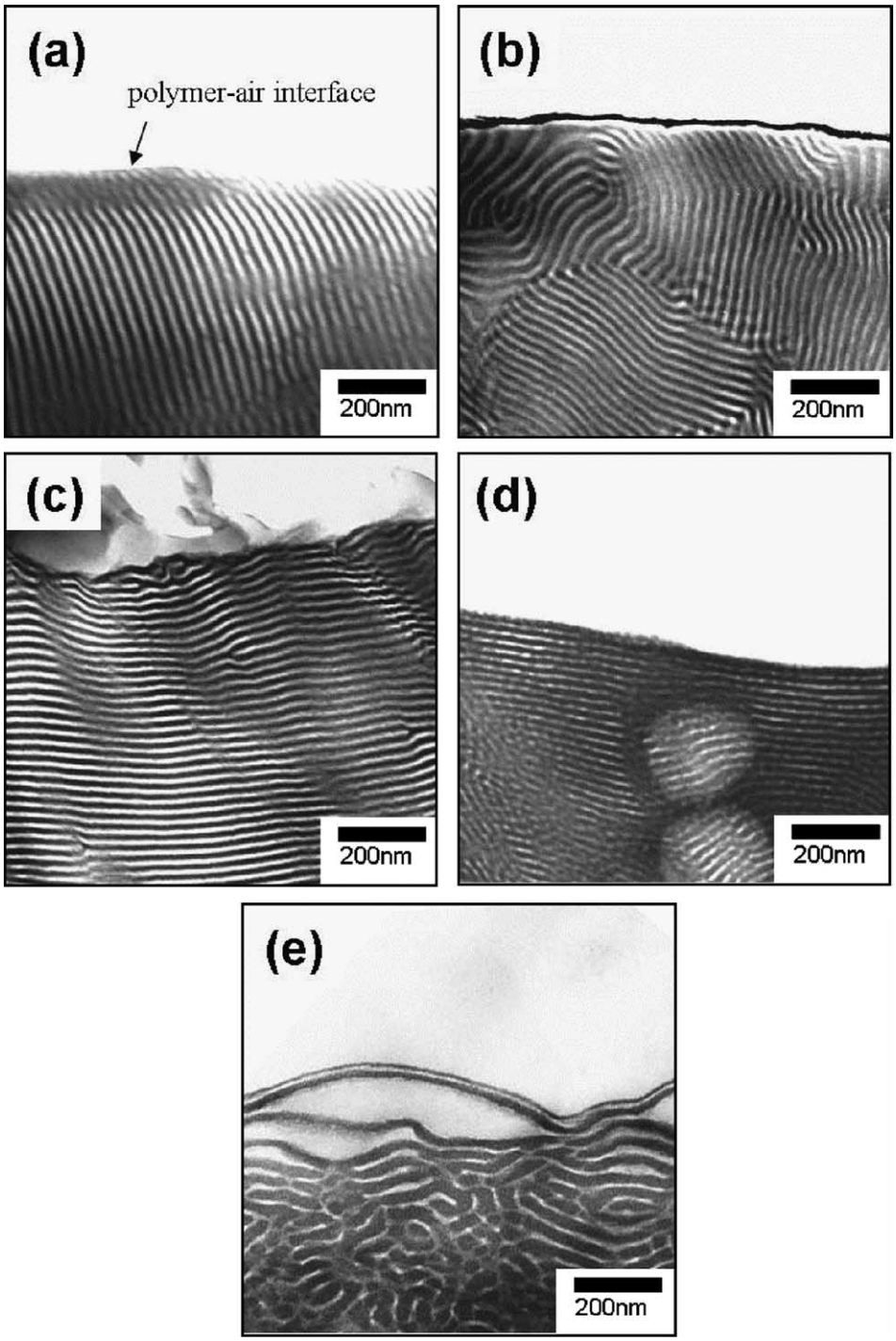

Fig. 4. Cross-sectional TEM morphologies of SBS and SBS/rosin films: (a) SBS, (b) 5 wt%, (c) 10 wt%, (d) 15 wt%, and (e) 20 wt% rosin blend, respectively.

condition for molecular ordering. In contrast to previous reports [15,16], the annealed SBS film displays PS cylinder orientation perpendicular to the surface (Fig. 4), which might be attributed to the kinetic effects observed during the process of solvent evaporation. This orientation in thicker SBS films (200 μm) remained unaltered even during thermal annealing at 120 °C for 4 days; conditions considered insufficient to induce mobility in the PS domains of the neat SBS film. Therefore, the perpendicular morphology is a consequence of kinetic trapping. Since, the mobility of the PS domains increases significantly as the rosin content increases, the near-surface orientation changes from perpendicular to parallel at 10 wt% rosin addition. This result correlates with the cylindrical to lamellar phase transition in the bulk observed in both the SAXS and TEM studies.

While similar lamellar orientation is maintained for SBS/rosin blends with 10–20 wt% rosin, the cross-sectional TEM micrographs of the SBS/rosin films revealed a different level of macrophase separation of the rosin near the surface, compared to the bulk. For the 10 wt% rosin blend, the near-surface

morphology had a parallel lamellar orientation without any significant rosin separation. While at 15 wt% rosin content, the rosin starts to form separated phases from the blends, presumably because the PS domains are saturated with rosin. In this case, the near-surface TEM micrographs showed that the rosin forms submicron spherical domains without disturbing the ordered lamellar domains of the SBS/rosin blend. This intermediate rosin phase is not indicated in the bulk TEM micrographs, and may in fact be a type of kinetic intermediate structure that forms when the rosin becomes separated near the surface. At 20 wt% rosin content, the rosin domains are clearly phase-separated on the micron scale and encapsulated by PS domains underneath the surface PB layer. Furthermore, the periodicity of the lamellar structure seemed to increase by a factor of 1.4. Considering the SAXS results, however, the lamellar domain spacing in the 20 wt% rosin blend should be similar to that observed in the 10 or 15 wt% blends. Therefore, the apparent increase in lamellar spacing observed in the cross-sectional TEM micrographs for the 20 wt% rosin blend might be attributed to artifacts induced by sample deformation during cutting. As such, the higher the rosin content in the blends, the softer the material is and the more difficult it is to microtome samples without any deformation.

3.3. Tack behavior of SBS/rosin blend films

Probe tack tests have been performed on solvent-cast SBS/rosin films, whose near-surface morphologies have been previously characterized by cross-sectional TEM. The adhesion energy is attributed to an additive combination of the intrinsic work of adhesion associated with the surface properties and the viscoelastic dissipation energy of the adhesives incurred by the deformation of the material [23].

Fig. 5 represents the probe tack forces determined for SBS/rosin films, when a circular probe of 5 mm diameter is pressed into the film and then withdrawn. In the case of probe tacks with large dissipation energies, the surface property contribution to the tack force is negligible, because a relatively large scale deformation is involved during the withdrawal of the probe, and the thickness of the uppermost PB layer is very small (i.e. <15 nm) (Fig. 4). Therefore, the large-scale (mm) tack force tests should depend on the near-surface morphology beyond the uppermost surface layer. The cylinder to lamellar morphology transition affects the tack behavior because of the preferential solubility of rosin in PS over the PB domains. Moreover, the morphology of perpendicular or parallel orientations is also known to affect the tack behavior. For the neat SBS film, the perpendicularly oriented PS domains are identified by TEM (Fig. 4(a)). The perpendicular glassy PS domains interfere with the PB domain deformation during the fast detaching of the probe. On the contrary, when the lamellar phases start to develop (Fig. 4(c)), the parallel orientation of the PS domains at the surface can induce larger deformations in the PB matrix compared to perpendicular PS domains. Therefore, it was inferred that an increase in the macro tack force should exist following the cylinder to lamellar transition. Instead, however, a maximum tack force was observed at 15 wt% rosin. Given that the parallel lamellar orientation is dominant between 10 and 20 wt% rosin, the maximum tack force matches with the onset of the macrophase separation of rosin at 15 wt%. The cross-sectional TEM micrograph obtained near the surface of the 15 wt% rosin blend shows that micron-sized domains exist and that they become superposed with the block copolymer microphase separation (Fig. 4(d)). It is believed these domains are weakly phase-separated rosins due to the limited rosin solubility. For the 20 wt% rosin blend, the effect of the rosin solubility limitation amplifies and induces the formation of a macroscopic hard rosin phase near the surface, resulting in a drastic decrease in the tack force.

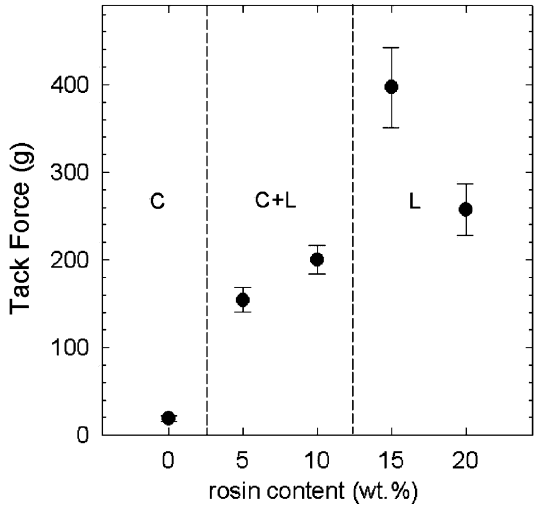

Fig. 5. Probe tack forces of solvent-cast SBS and SBS/rosin thin films (200 μm) as a function of the rosin content (contact force: 100 g, contact time: 10 s, pulling rate: 10 mm/s).

4. Summary and conclusions

Correlations between the near surface morphology and the tack behavior of SBS/rosin ester blends have been studied using tack probes at different length scales. The rosin ester ($T_g \sim 50$ °C) was selectively soluble in the PS domains, and the addition of rosin to SBS increased the composition of 'PS + rosin' domains. As the rosin content in the SBS/rosin blends was increased, the coexisting cylinder and lamellar phases, together with the corresponding cylinder to lamellar phase transition in the SBS/rosin bulk, were clearly evident in both the SAXS and TEM studies. The air-polymer surface was covered with a PB layer, as confirmed by TEM. As the rosin content in the SBS/rosin blends was increased beyond 10 wt%, the near-surface morphologies changed from a perpendicular to a parallel orientation.

In macro-probe tack tests using a 5 mm diameter metal probe, due to the large probing area, the probe tack force displayed a strong correlation with the near-surface morphology. As rosin was added to the SBS, the probe tack force showed a steady increase. The near surface domain orientations changed from perpendicular cylinder to parallel lamellae at 10 wt% rosin, which is probably associated with the deformation ability of the subsurface layers. While parallel

lamellar orientations at the surface were observed in the SBS/rosin blends between 10 and 20 wt% rosin, the cross-sectional TEM micrographs revealed weakly phase-separated rosin domains at 15 wt% rosin. It is believed that this morphological feature is responsible for the observed macro tack force maximum at 15 wt% rosin.

Acknowledgements

The authors thank the Ministry of Science and Technology of Korea (National Research Laboratory Program) and the Ministry of Education of Korea (BK21 Program), the Advanced Environmental Biotechnology Research Center at Pohang University of Science and Technology, the Regional Technology Innovation Program (grant No. RT104-01-04) of the Ministry of Commerce, Industry, and Energy for their financial support, and the Pohang Accelerator Laboratory for providing the 4C1 beam line used in this study.

References

[1] Galan C, Sierra CA, Fatou JMG, Delgado JA. J Appl Polym Sci 1996;62:1263.
[2] Tse MF. J Adhes Sci Technol 1989;3:551.
[3] Tse MF, Jacob L. J Adhes 1996;56:79.
[4] Class JB, Chu SG. J Appl Polym Sci 1998;30:805.
[5] O'Connor AE, Macosko CW. J Appl Polym Sci 2002;86:3355.
[6] Crosby AJ, Shull KR. J Polym Sci, Part B: Polym Phys 1999;37:3455.
[7] Pocius AV. Rubber Chem Technol 1985;58:622.
[8] Satas D. Handbook of pressure sensitive adhesive technology and application. Warwick: Satas and Associates; 2002 [p. 36].
[9] Creton C, Hooker J, Shull KR. Langmuir 2001;17:4948.
[10] Paiva A, Foster MD, Von Meerwall ED. J Polym Sci, Part B: Polym Phys 1998;36:373.
[11] Kim JW, Han CD, Chu SG. J Polym Sci, Part B: Polym Phys 1988;26:677.
[12] Aubrey DW, Sherriff M. J Polym Sci, Part A: Polym Chem 1980;18:2597.
[13] Vandijk MA, Vandenborg R. Macromolecules 1995;28:6773.
[14] Sakurai S, Sakamoto J, Shibayama M, Nomura S. Macromolecules 1993;26:3351.
[15] Turturro A, Gattiglia E, Vacca P, Viola GT. Polymer 1995;36:3987.
[16] Kim G, Libera M. Macromolecules 1998;31:2569.
[17] Hasegawa H, Hashimoto T. Polymer 1992;33:475.
[18] Thomas HR, Omalley JJ. Macromolecules 1979;12:323.
[19] Varma R, Takeichi H, Hall JE, Ozawa YF, Kyu T. Polymer 2002;43:4667.
[20] Fox TG. Bull Am Phys Soc 1956;1:126.
[21] Lodge TP, Pudil B, Hanley KJ. Macromolecules 2002;35:4707.
[22] Liu Y, Zhao W, Zheng X, King A, Singh A, Rafailovich MH, et al. Macromolecules 1994;27:4000.
[23] Gent AN, Shultz J. J Adhes 1972;3:281.